Journal of the European Ceramic Society 16 (1996) 1253–1262

PII:S0955-2219(96)00049-0
0955-2219/96/$15.00

Influence of Zirconia Addition on the Crystallization Kinetics of a Y–Si–Al–O–N Glass

P. Vomacka,[a] R. Ramesh[b] & S. Hampshire[b]

[a] Department of Engineering Materials, Luleå University of Technology, S-951 87 Luleå, Sweden
[b] Materials Research Centre, University of Limerick, Limerick, Ireland

(Received 13 December 1995; revised version received 14 February 1996; accepted 20 February 1996)

Abstract

The crystallization behaviour of YSiAlON glasses with and without ZrO_2 additives, prepared by melting at 1700°C, were studied by means of differential scanning calorimetry, scanning microscopy and X-ray powder diffraction analysis. The optimum nucleation temperatures were determined to be T_g + 65°C and T_g + 50°C for the ZrO_2-free and the ZrO_2-containing glass, respectively. The crystallization of the glasses was found to be dominated by the surface mechanism of nucleation and growth. The added zirconia acted as a growth modifier rather than a nucleating agent. Copyright © 1996 Elsevier Science Ltd

1 Introduction

Silicon nitride based ceramics contain oxynitride glass phases at the grain boundaries that control the high-temperature properties and subsequent behaviour. The desire to understand the nature of these grain boundary phases has resulted in a number of investigations on oxynitride glass formation and properties.[1–5] Much of the earlier interest centred largely on the influence of nitrogen, which in silicate glasses increases their viscosity, glass transition temperature and hardness.[3–5] Further, the improvement obtained in the thermomechanical properties of Si_3N_4 ceramics following crystallization of the grain boundary oxynitride glass[6,7] has prompted more detailed work on the microstructure and crystallization behaviour of bulk materials similar to the glass phases present at the grain boundaries of these ceramics. Such studies have been largely carried out in the YSiAlON system[8–10] since Y_2O_3 and Al_2O_3 have proven to be effective additives for Si_3N_4 ceramics.

Control of nucleation is extremely important in the formation of glass-ceramics. The crystalline phases formed on heat treatment and the extent of their formation will determine the properties of the particular material. The phases formed depend on both the composition of the parent glass and the heat treatment process. Some glasses require the addition of a nucleating agent to promote crystallization. The YSiAlON glasses, in general, appear to be self-nucleating.[9–11] However, Thomas *et al.*[12] observed improved crystallization behaviour for an oxynitride glass containing a small addition of ZrO_2. Furthermore, Braue *et al.*[13] found a significant improvement of high-temperature strength of (Y_2O_3 + Al_2O_3) fluxed sintered Si_3N_4 partially doped with small amount of ZrO_2. In contrast, the work of Cheng and Thompson[14] and Shaw *et al.*[15] on zirconia additions to nitrogen ceramics show no appreciable improvements in mechanical properties and this has been attributed to the difficulty of retaining transformable ZrO_2 in this system.

In previous studies[16,17] on yttria–alumina–silica glasses with addition of zirconia as a nucleating agent, zirconia was considered to act as a growth modifier rather than a catalyst nucleating agent. The solubility limit of zirconia in a YSiAlO melt at 1700°C was found to be 6 wt%. In the present work, the influence of ZrO_2 addition on the crystallization kinetics of an oxynitride glass prepared at 1700°C is studied. The crystallization mechanisms, the optimum nucleation temperatures and the activation energies for the crystallization process in ZrO_2-free and ZrO_2-containing compositions are compared by means of differential scanning calorimetry (DSC), scanning electron microscopy (SEM) and X-ray powder diffraction analysis. The Y:Si:Al ratio (in equivalent %) chosen for the oxynitride glass in the present investigation is the same as in the previously studied oxide glass.[16] Nitrogen (10 equivalent %) is incorporated into the oxide composition to form the oxynitride glass.

2 Experimental

2.1 Glass preparation

A YSiAlON glass of composition (in equivalent %) 27Y:42Si:31Al:90O:10N without ZrO_2 and one

with the addition of 6 wt% monoclinic ZrO_2 (Sigma Chemical) was prepared from mixtures of silicon nitride (KemaNord Industrikemi), high-purity yttria, alumina and silica (Rhone Poulenc, Alcoa Chemicals, Johnson Matthey) in the appropriate proportions. The equivalent % method of representation of composition has been reported previously.[18] The powders were mixed in polyethylene containers on a Siemens roller mill for 10 h using propanol as mixing medium. The alcohol was then evaporated and the powder mixtures were sieved. Batches of approximately 100 g each were then mechanically compacted into molybdenum crucibles and melted under 0.17 MPa nitrogen at 1700°C for 2·5 h, after which the melt was rapidly cooled down to 880°C and then annealed at this temperature for 1 h prior to slow furnace cooling.

2.2 Glass characterization

To study quality and homogeneity, observations on melting and final appearance were made. X-ray analysis was carried out using a Philips X-ray powder diffractometer (Cu K_α radiation) in order to detect any crystalline phases present in the glasses. SEM analysis was carried out using a Jeol 840 scanning electron microscope to assess homogeneity. The densities were measured by Archimedes' principle using water as the working fluid. Microhardness was obtained using a Vickers indentor with a load of 300 g applied for 15 s. A Stanton-Redcroft differential scanning calorimeter was used to determine glass transition (T_g) and crystallization (T_c) temperatures. Similar characterization techniques were employed for the glass-ceramics obtained after two-stage heat treatments in the tube furnace.

2.3 Heat treatments using DSC for optimum nucleation temperature determination

Differential scanning calorimetry was performed on the glasses to determine the optimum nucleation temperature using the method outlined by Marotta *et al.*[19] The relationship between the number of nuclei N_n and the time t_n of nucleation heat treatment is given by:

$$N_n = It_n^b \quad (1)$$

where I is the kinetic rate constant of nucleation and b is a parameter related to the nucleation mechanism. If the samples are held for the same time t_n at each temperature T_n of the heat treatment, then the following equation applies:

$$\ln I = (E_c/R)(1/T_p - 1/T_{p'}) + \text{constant} \quad (2)$$

where E_c is the activation energy for crystallization, R is the gas constant, T_p and $T_{p'}$ are the crystallization exotherm temperatures obtained after and without a nucleation hold, respectively. The factor $(1/T_p - 1/T_{p'})$ has been shown to be a function of T_n, the nucleation hold temperature, and a plot between them gives a bell-shaped curve, the maximum of which is the temperature at which optimum nucleation occurs.[19]

Small quantities of powdered glass samples of particle size 53 to 90 μm were held in boron nitride lined platinum crucibles and alumina was used as a reference material. These were then heated at 20°C min^{-1} in a flowing nitrogen atmosphere to temperatures ranging between T_g (glass transition temperature) and T_g + 100°C for 1 h, after which heating was continued at 10°C min^{-1} until the crystallization peak (T_{c2}) was observed. The reason for choosing the T_{c2} peak will become apparent later. From the DSC traces the peak temperatures of crystallization corresponding to the different nucleation hold temperatures were recorded. Prior to these experiments, an initial DSC run was carried out without a nucleation hold and this was used as a reference for determining the shift in crystallization peaks resulting from the nucleation treatment in the other runs. The isothermal heat treatment that resulted in the greatest depression in crystallization temperature is taken as the optimum nucleation temperature.

The activation energy for the crystallization process was determined using the method of Matusita and Sakka[20] on the basis that the crystallization of glass is advanced by a nucleation and growth mechanism. The method involves DSC runs performed at several heating rates and subsequent analysis of variation of peak temperature with heating rate. Five different heating rates (5, 8, 10, 15 and 20°C min^{-1}) were employed, maintaining the same particle size (53 to 90 μm). The relationship between heating rate and exothermic peak temperature is given by:

$$\ln(\alpha^n/T_p^2) = -m\,E_c/RT_{p'} + \text{constant} \quad (3)$$

where α is the heating rate, $T_{p'}$ the maximum crystallization exothermic peak temperature, E_c the activation energy for crystallization, R is the gas constant and n and m are numerical constants which depend on the crystallization mechanism ($n = m = 1$ for surface-dominated nucleation and $n = m = 3$ for bulk crystallization from a constant number of nuclei[21]). In order to determine the mechanism of crystallization, i.e. whether crystallization proceeds by bulk or surface nucleation, additional DSC runs were carried out under identical conditions on three samples of varying particle sizes for both glass compositions. Considering the nucleation process as surface-dominated, as

will be seen below, the values of $\ln(\alpha/T_p^2)$ were determined and plotted against $1/T_p$. The resulting slope was used to calculate the activation energy (E_c).

2.4 Heat treatments in tube furnace

A two-stage heat treatment was carried out in a nitrogen atmosphere using a tube furnace. Coupons (10 mm × 10 mm × 2 mm) cut from these glasses were placed in a bed of boron nitride in an alumina crucible in a tube furnace and heat-treated at the optimum nucleation temperature (determined using DSC) for 10 h, followed by a treatment at the crystal growth temperature for 30 min. Crystal phases of the heat-treated specimens were analysed by X-ray diffraction, and both surface and sectioned morphologies observed using scanning electron microscopy on diamond-polished sections without etching.

3 Results

3.1 Glass characterization

Table 1 shows the X-ray analysis and observations on melting for both ZrO_2-free and ZrO_2-containing glass compositions. As can be seen, both compositions gave fully amorphous material. However, a slight difference was observed with regard to their appearance. The ZrO_2-free composition produced a faint yellow transparent glass while the ZrO_2-containing composition gave a yellowish grey transparent glass. Further, SEM analysis indicated glasses to be homogeneous. Some of the physical properties obtained on the as-melted compositions are summarized in Table 2. The minimum point in the endothermic drift of the DSC curves (Fig. 1) corresponding to the end of the transition range is reported as the glass transition temperature (T_g) in Table 2, while T_{c1} and T_{c2}

Table 1. Characterization of as-melted glass compositions

Composition (eq%)	*X-ray analysis*	*Observations on melting*
27Y:42Si:31Al:90O:10N	Amorphous	faint yellow transparent glass
27Y:42Si:31Al:90O:10N + 6 wt% ZrO_2	Amorphous	yellowish grey transparent glass

Table 2. Physical properties of as-melted glass compositions

Composition (eq%)	T_g *(°C)*	T_{c1} *(°C)*	T_{c2} *(°C)*	*Density (g cm^{-3})*	*Hardness (GPa)*
27Y:42Si:31Al:90O:10N	952	1 106	1 238	3·60	10·21 ± 0·35
27Y:42Si:31Al:90O:10N + 6 wt% ZrO_2	945	1 116	1 245	3·65	10·46 ± 0·4

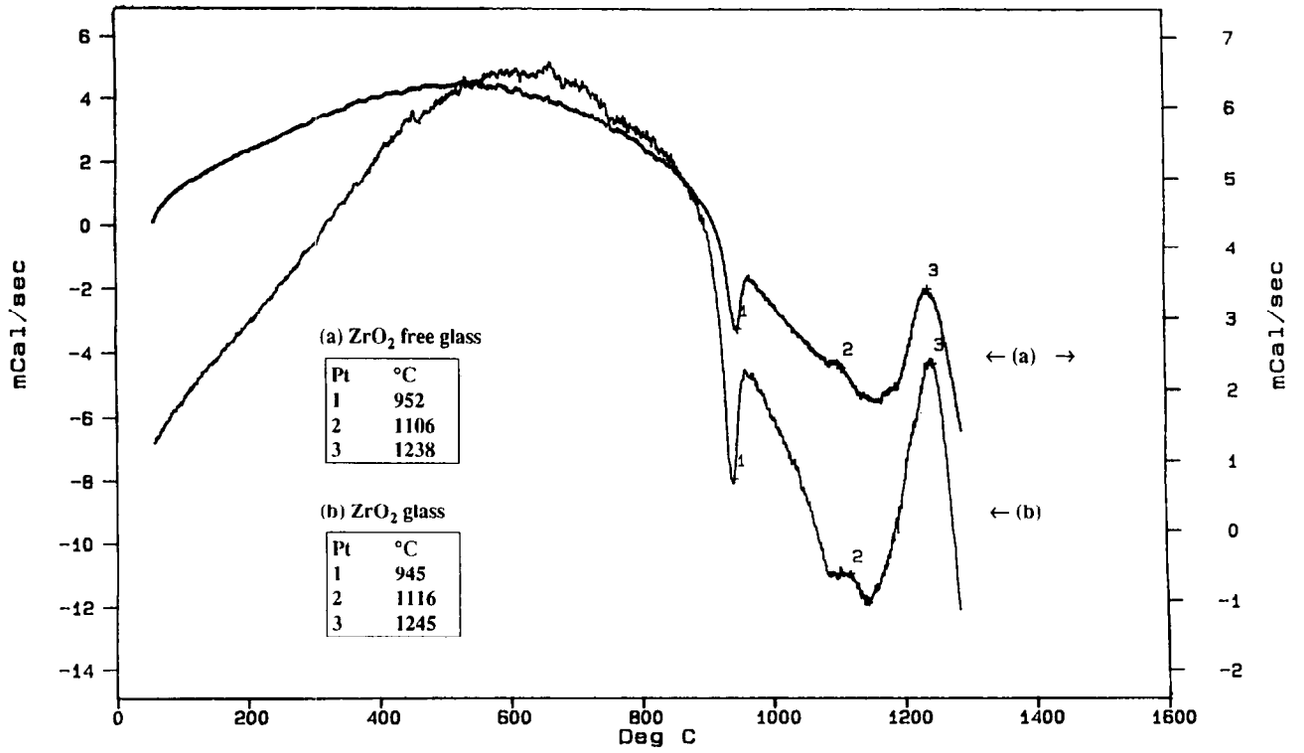

Fig. 1. Non-isothermal DSC traces for YSiAlON glasses (a) without ZrO_2 and (b) with ZrO_2.

are the first and second crystallization exotherm temperatures, respectively, obtained from the maxima of the exothermic peaks. From these results it can be seen that zirconia addition slightly shifts the T_g to lower temperatures and crystallization peaks (T_{c1} and T_{c2}) to higher temperatures. Further, from the DSC curves shown in Fig. 1 it can be seen that, for both glass compositions, exothermic peaks corresponding to T_{c1} are rather weak while those corresponding to T_{c2} are sharp and distinct. Because of this, the shift in the T_{c2} peak was monitored below to determine the optimum nucleation temperature and the activation energy for crystal growth. With regard to other properties, the density and the hardness values were slightly higher for the ZrO_2-containing glass composition.

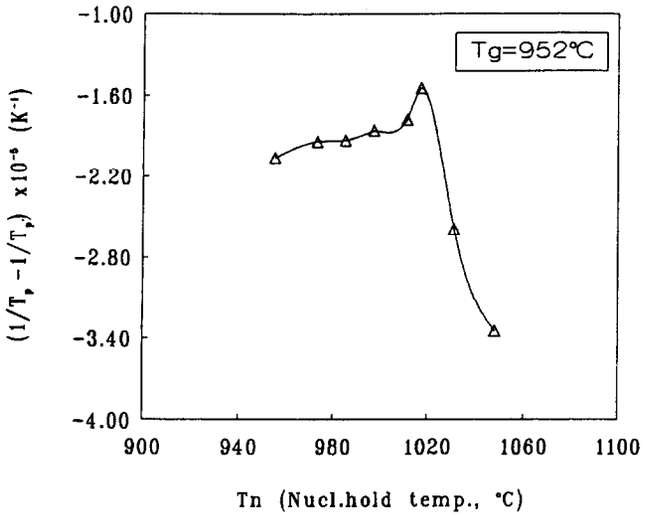

Fig. 2. Nucleation rate–temperature curve for ZrO_2-free YSiAlON glass.

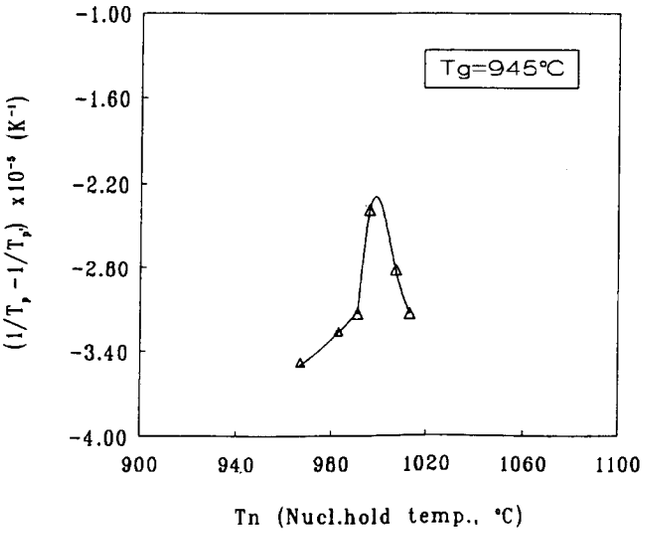

Fig. 3. Nucleation rate-temperature curve for ZrO_2-containing YSiAlON glass.

3.2 Heat treatments using DSC for optimum nucleation temperature determination

The $(1/T_p - 1/T_{p'})$ versus nucleation hold temperature (T_n) plots obtained from the peak shifts measured on the DSC traces are shown in Figs 2 and 3 for ZrO_2-free and ZrO_2-containing YSiAlON glass compositions, respectively. Table 3 summarizes the results of these plots. As can be seen, for the glass without ZrO_2 the maximum nucleation occurs at 1017°C, corresponding to T_g + 65°C, while for the ZrO_2-containing glass it occurs at 995°C, which corresponds to T_g + 50°C. Another observation is that the slope of the left side of the curve for the ZrO_2 glass is steeper compared with that for the ZrO_2-free glass, which indicates that maximum nucleation occurs closer to the glass transition temperature for the ZrO_2-containing glass.

In order to determine the activation energy for crystallization, the mechanism of crystallization, i.e. whether crystallization proceeds by bulk or surface nucleation, should be taken into account. For this purpose, additional non-isothermal DSC runs with a heating rate of 15°C min^{-1} were carried out on three samples of varying particle sizes. The exothermic peak temperatures (T_{c2}) obtained from DSC traces of these experiments are shown in Table 4. It can be seen that as the particle size increases the crystallization peaks are shifted to higher temperatures for the same heating rate (15°C min^{-1}) for both compositions. This variation in exothermic peak temperature with varying particle sizes is indicative of a surface nucleation mechanism.

Figures 4 and 5 respectively show the activation energy plots obtained using the Matusita method for the ZrO_2-free and ZrO_2-containing glass compositions. The activation energy for crystallization was calculated from the slope of these straight lines according to eqn (3) taking $n = m = 1$ for surface-dominated nucleation. The values thus obtained are 365 kJ mol^{-1} for the ZrO_2-free glass and 280 kJ mol^{-1} for the ZrO_2-containing glass. Without emphasizing the actual magnitudes of these values too much, it is pertinent to note that the addition of ZrO_2 lowers the activation energy for crystallization.

Table 3. Optimum nucleation temperatures obtained using DSC technique

Composition (eq%)	T_g(°C)	*Opt. nucleation temperature*
27Y:42Si:31Al:90O:10N	952	T_g + 65°C
27Y:42Si:31Al:90O:10N + 6 wt% ZrO_2	945	T_g + 50°C

Table 4. Crystallization temperatures (T_{c2} in °C) obtained for both glass compositions of varying particle size

Composition (eq%)	*Particle size*		
	<53 μm	*53–90 μm*	*>150 μm*
27Y:42Si:31Al:90O:10N	1198	1238	1257
27Y:42Si:31Al:90O:10N + 6 wt% ZrO_2	1202	1245	1266

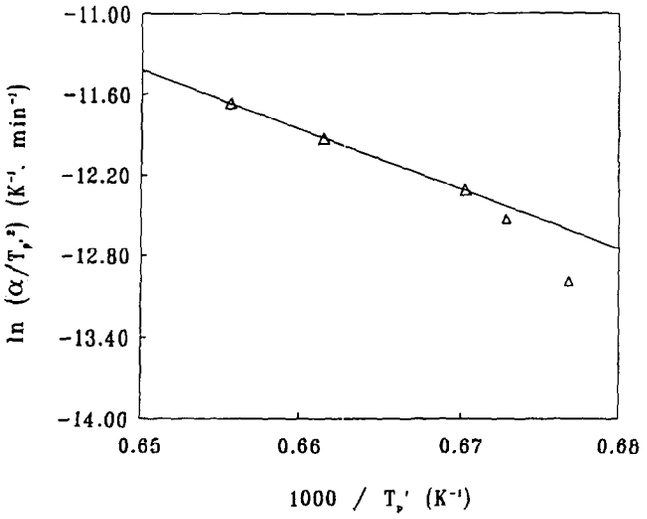

Fig. 4. Activation energy plot for the crystallization process occurring in ZrO_2-free YSiAlON glass.

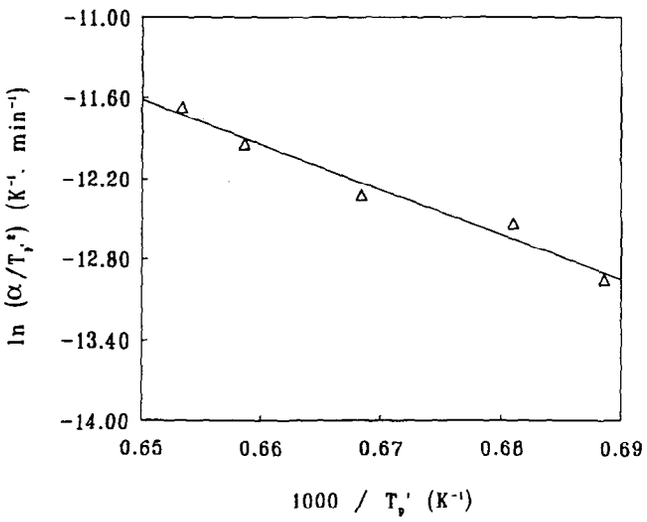

Fig. 5. Activation energy plot for the crystallization process occurring in ZrO_2-containing YSiAlON glass.

3.3 Tube furnace experiments

Both glasses were subjected to two-stage heat treatments employing a tube furnace at temperatures corresponding to optimum nucleation and crystal growth. Thus the schedule for the heat treatment of the ZrO_2-free composition involved a nucleation treatment at T_g + 65°C (1017°C) for 10 h followed by a crystallization treatment at 1230°C for 30 min. For the ZrO_2-containing glass, a nucleation treatment for 10 h was given at a temperature corresponding to T_g + 50°C (995°C), followed by a crystallization treatment at 1220°C. The chosen crystal growth temperatures correspond to the exotherm temperatures observed in DSC (Figs 6 and 7) during the nucleation hold at the respective temperatures.

Phase assemblages of the heat-treated glass samples identified by X-ray diffraction (Table 5) include yttrium disilicate ($Y_2Si_2O_7$) and $Y_4Al_2O_9$ (YAM) as the major crystalline phases and also traces of mullite ($Al_6Si_2O_{13}$). For the ZrO_2-containing glass, yttrium disilicate exists in both β and γ polymorphs while only the β form was observed for the ZrO_2-free glass. In addition, for the ZrO_2-containing glass, cubic yttria-stabilized ZrO_2 ($Y_{0.15}Zr_{0.85}O_{1.93}$) was noted.

The surface and sectioned morphologies of the glass-ceramic microstructures obtained following two-stage heat treatments at temperatures corresponding to optimum nucleation and crystal growth are shown in Figs 8 and 9 for ZrO_2-free and ZrO_2-containing glass, respectively. The morphologies of both glass-ceramics are dendritic in nature with crystals being relatively coarser for ZrO_2-containing glass-ceramic. The small bright crystals seen in the surface micrograph of ZrO_2-containing glass-ceramic are yttria-stabilized ZrO_2 crystallizing out from the parent glass as XRD analysis would indicate. Further, for both glass-ceramics, examination of the sectioned morphologies [Figs 8(b) and 9(b)] reveal much lower volume fraction crystallization compared with the surface layers. This indicates the predominance of surface nucleation for these glass-ceramics and is in good agreement with the DSC results mentioned above (Table 4).

The results of the additional characterization carried out on heat-treated specimens of both compositions are summarized in Table 6. Devitrification of both glasses produced dark grey coloured glass-ceramics and these were opaque in nature. Comparing Tables 2 and 6 it can be seen that there is a slight decrease in density and an increase in hardness after crystallization in both glass compositions. The ZrO_2-containing glass and glass-ceramic are marginally harder than the ZrO_2-free composition.

4 Discussion

The glass transition temperature of the as-prepared oxynitride glasses determined in this study

are higher than the values obtained on the corresponding oxide glasses.[16,17] This increase is attributed to the incorporation of nitrogen into the glass structure leading to a more rigid glass network, as reported elsewhere.[4,5]

Though small, there exists a difference in the physical properties of YSiAlON glasses with and without ZrO_2 additives (Table 2). It is interesting to note that zirconia addition shifts T_g to a slightly lower temperature and it is assumed that the addition of ZrO_2 causes a decrease in viscosity of the glass. Crystallization temperatures (T_{c1} and T_{c2}) move to higher values and, from a thermodynamic point of view, this is feasible since an additional component would lead to an increase in the entropy of the system, thereby hindering crystal-

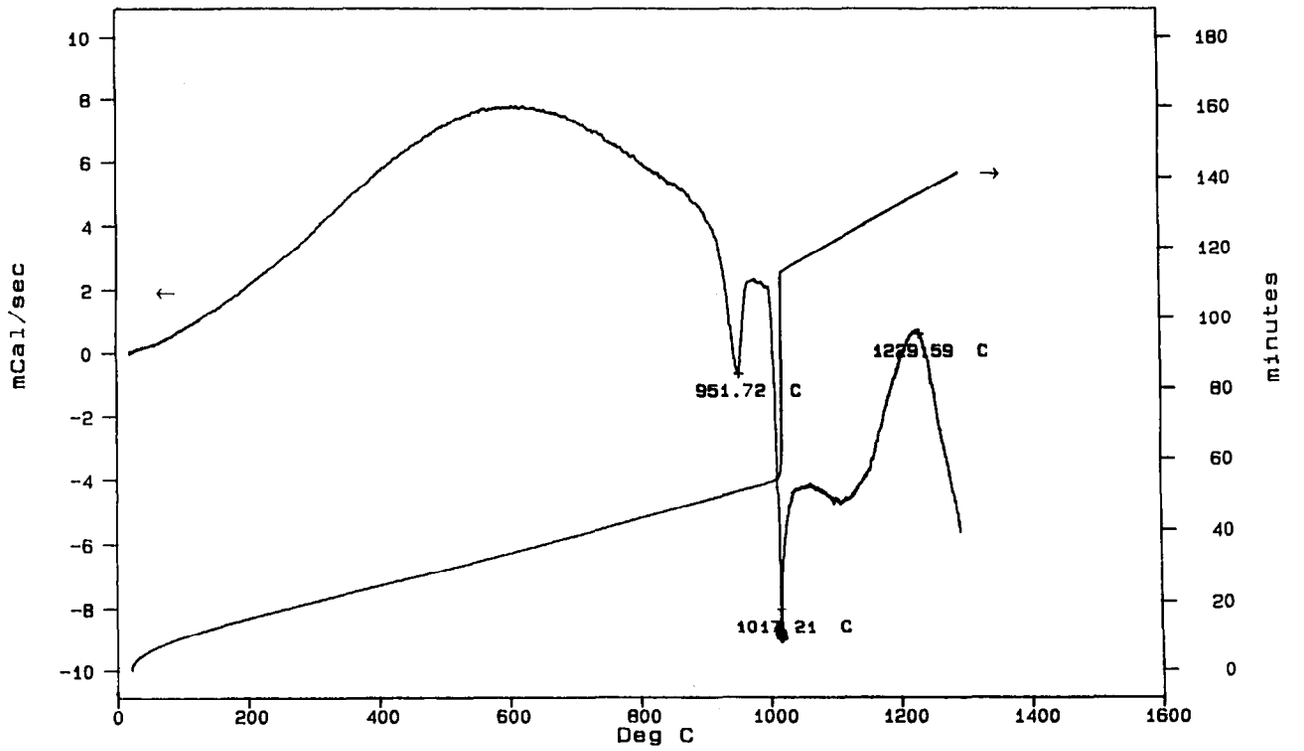

Fig. 6. DSC trace of ZrO_2-free glass obtained following the isothermal test carried out at T_g + 65°C.

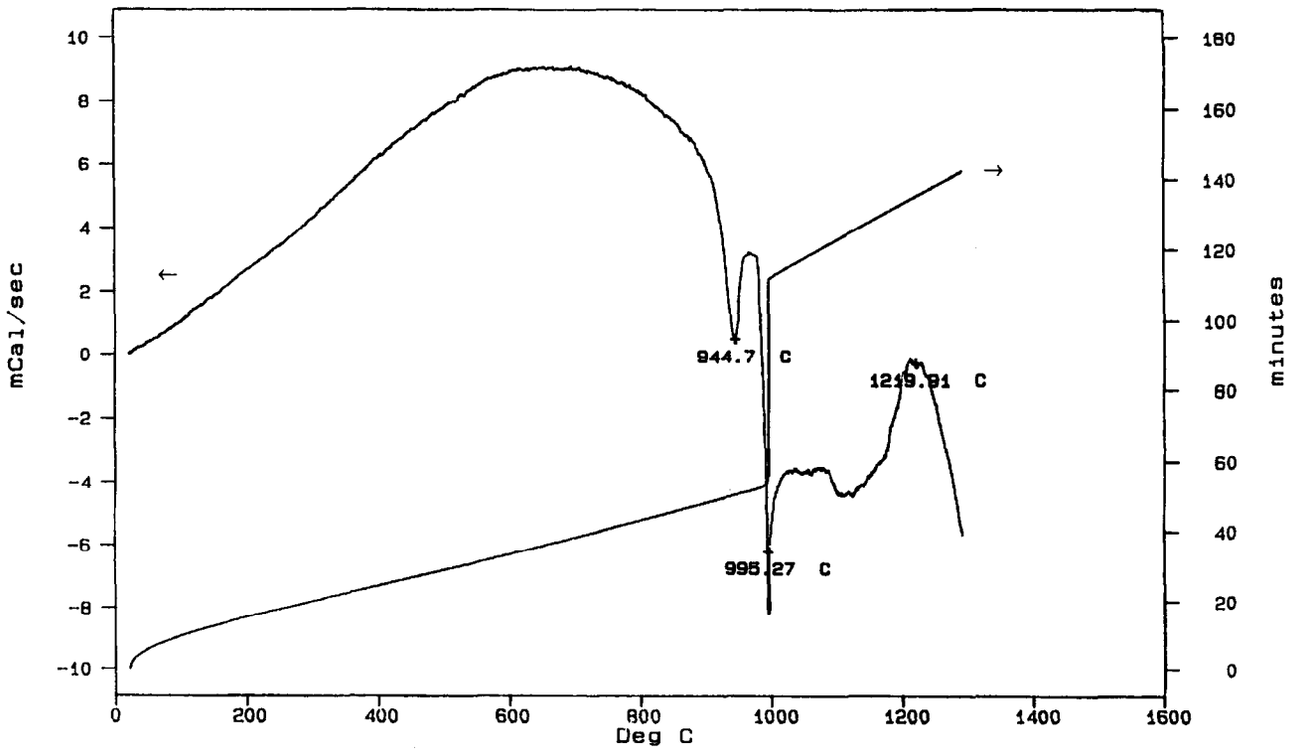

Fig. 7. DSC trace of ZrO_2-containing glass obtained following the isothermal test carried out at T_g + 50°C.

lization. The increase in density and hardness observed for the ZrO_2-containing glass can perhaps be attributed to higher nitrogen retention during melting than for the glass without the additive. This argument is based on the fact that nitrogen has a higher affinity towards zirconia and that nitrogen itself can be incorporated into the zirconia structure.[14,15,22]

The optimum nucleation temperatures for the ZrO_2-free and ZrO_2-containing glasses, derived from the DSC data in Figs 2 and 3, are 1017°C (T_g + 65°C) and 995°C (T_g + 50°C), respectively. These temperatures correspond to the maximum in the ($1/T_p$ - $1/T_{p'}$) versus T_n curve. Thus it is evident that the optimum nucleation temperature is lowered by the addition of ZrO_2, with the highest nucleation rate closer to the glass transition temperature for the ZrO_2-containing glass. However, for both glasses the crystallization process seems to depend on the specific surface area of the glass samples used in the DSC experiments (Table 4). For samples of high specific surface area (<53 μm), the crystals grow from a large number of surface nuclei and consequently lower T_{c2} values

Table 5. Crystalline phases observed after two-stage heat treatment for both glass compositions

Composition (eq%)	*Phase assemblage*
27Y:42Si:31Al:90O:10N	β–$Y_2Si_2O_7$, $Y_4Al_2O_9$, $Al_6Si_2O_{13}$[a]
27Y:42Si:31Al:90O:10N + 6 wt% ZrO_2	γ–$Y_2Si_2O_7$, β–$Y_2Si_2O_7$, $Y_4Al_2O_9$, $Y_{0.15}Zr_{0.85}O_{1.93}$, $Al_6Si_2O_{13}$[a]

[a] Trace amounts.

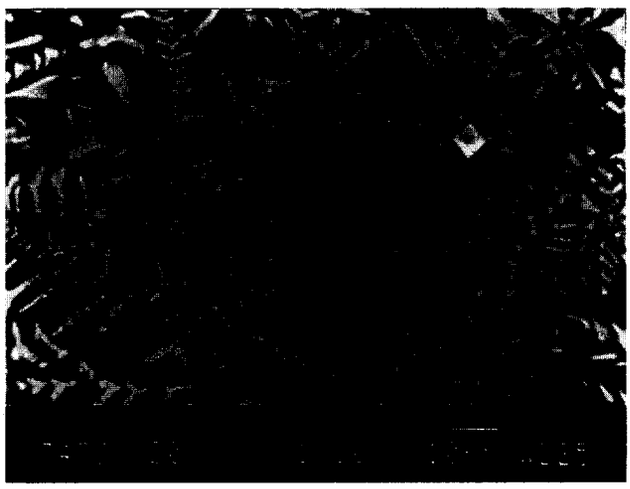

(a)

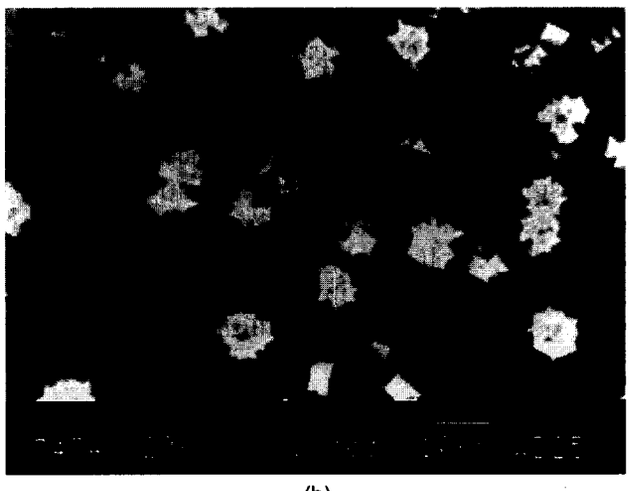

(b)

Fig. 8. Micrographs of ZrO_2-free YSiAlON glass obtained following two-stage heat treatments (1017°C for 10 h, 1230°C for 30 min): (a) surface morphology and (b) sectioned morphology.

(a)

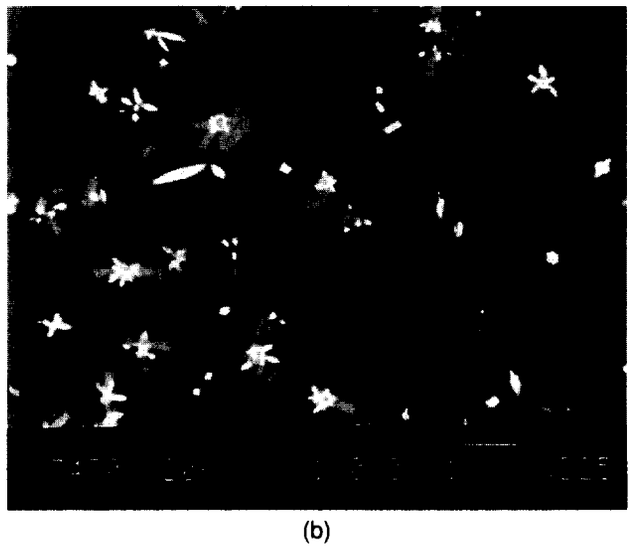

(b)

Fig. 9. Micrographs of ZrO_2-containing YSiAlON glass obtained following two-stage heat treatments (995°C for 10 h, 1220°C for 30 min): (a) surface morphology and (b) sectioned morphology.

were observed. As the particle size increases, due to the lower specific surface area of the sample, the number of surface nuclei decreases and if surface nucleation is dominant, then, given the constant heating rate used in the DSC experiments, the T_{c2} peak should be shifted to higher temperatures. This was indeed the case observed for both glass compositions. The difference observed in the shape of the $(1/T_p - 1/T_{p'})$ versus T_n curves (Figs 2 and 3) can then be said to simply imply that a significant nucleation occurs over a much narrower temperature interval for the ZrO_2-containing glass compared with the ZrO_2-free glass. However, from the SEM analysis, some bulk nucleation had occurred to a limited extent, possibly associated with the presence of Fe/Si impurity particles in the glass or with the precipitated ZrO_2 crystals.

The surface morphologies of both glass-ceramics after the two-stage heat treatment in the tube furnace are of dendritic appearance (Figs 8 and 9). However, the crystals are relatively coarser for the ZrO_2-containing glass-ceramic. This implies that the crystal growth on the surface proceeds from a smaller amount of nuclei for the ZrO_2-containing glass than for the ZrO_2-free glass. The sectioned morphology of the ZrO_2-free glass-ceramic [Fig. 8(b)] consists mainly of spherulites of the $Y_2Si_2O_7$ phase, which indicates a rapid growth of the $Y_2Si_2O_7$ crystals during the crystal growth treatment. Similar spherulitic appearance of $Y_2Si_2O_7$ phase was observed in the previous study[16] on the crystallization behaviour of the pure oxide compositions in the ZrO_2-free glass. The sectioned morphology of the ZrO_2-containing glass-ceramic is somewhat different [Fig. 9(b)] and consists of mainly yttria-stabilized ZrO_2 and fine platelet-like $Y_2Si_2O_7$ crystals. It is rather interesting to note that $Y_2Si_2O_7$ crystals appear to be embedded in the region where zirconia is crystallizing out from the parent glass. This seems to suggest that ZrO_2 may provide heterogeneous nucleation sites for additional crystallization to take place. However, sectioned morphologies reveal much lower volume fraction crystallization compared with the surface layer and, in fact, this is similar to that observed for the ZrO_2-free glass, suggesting that ZrO_2 crystals do not act as heterogeneous nucleation sites.

To determine the activation energy for crystallization, the mechanism of crystallization must be known in order to apply eqn (3) correctly, i.e. to substitute correct values for the constants m and n. Based on the non-isothermal DSC runs (T_{c2} variation with particle size) and the sectioned morphologies obtained on the tube furnace heat-treated samples, it was assumed that surface crystallization is the dominant mechanism for both glass-ceramics and therefore values of $n = m = 1$ were considered appropriate. For the ZrO_2-free glass only three experimental values, corresponding to the heating rates of 20, 15 and 10°C min^{-1}, were used to determine the slope of the plot of $\ln(\alpha/T_{p'}^2)$ versus $1/T_{p'}$ in Fig. 4 and subsequently to estimate the activation energy of crystallization. This is because at the low heating region there appears to be a significant contribution of bulk crystallization as evident from the deviation from a linear plot. For the ZrO_2-containing glass, all the experimental data were taken into account for estimating the activation energy since no significant deviation from the straight line at the region of low heating rate was observed (Fig. 5), implying no appreciable contribution of bulk crystallization (mainly of yttria-stabilized zirconia) to the overall crystallization. The activation energy for crystallization process thus determined indicated a lower value (280 kJ mol^{-1}) for the ZrO_2-containing glass than for the ZrO_2-free glass (365 kJ mol^{-1}). It has to be stressed that the activation energies so obtained using variable heating rate methods are 'apparent' activation energies and may be the compound result of a number of simultaneous events, e.g. crystallization of more than one phase.[21] Nevertheless, these data are useful as aids in determining overall trends in crystallization behaviour.

The properties of the heat-treated glass-ceramics indicate a slight decrease in density and an increase in hardness after crystallization in both glass compositions (Tables 2 and 6). While the hardness improvement can be attributed to the devitrification process, the synergistic observation of a decrease in density and an increase in hardness seems to suggest the occurrence of a volume expansion as a result of crystallization. Zirconia additions increase the hardness only marginally. It should be emphasized that the objective of the present study was to investigate the influence of ZrO_2 addition on the crystallization process and

Table 6. Physical characterization of glass-ceramics

Composition (eq%)	*Appearance*	*Density ($g\ cm^{-3}$)*	*Hardness (GPa)*
27Y:42Si:31Al:90O:10N	dark grey opaque material	3·45	12·46 ± 0·6
27Y:42Si:31Al:90O:10N + 6 wt% ZrO_2	dark brown opaque material	3·48	12·68 ± 0·55

not to establish the optimum morphology in terms of maximum volume fraction crystallization from the parent glass. Therefore no attempts were made to optimize the crystal growth temperature and the duration of either the nucleation or the crystal growth treatments with respect to the maximum volume fraction crystallized as reported by Ramesh *et al.*[11] in an earlier study. Consequently, the hardness values of the glass-ceramics reported in Table 6 may not perhaps be the highest values possible.

With regard to the role of zirconia during the devitrification process, the following points should be noted. The XRD results reported in Table 5 reveal the crystalline phase assemblage in the ZrO_2-containing glass-ceramic to be more complex than in the ZrO_2-free glass-ceramic, with more different phases crystallizing from the parent glass. Cubic zirconia is stabilized by Y_2O_3 as revealed by the presence of $Y_{0.15}Zr_{0.85}O_{1.93}$ phase and this is completely crystallized easily from the parent glass accounting for the overall lower activation energy for crystallization.

Since there are no nitrogen-containing crystalline phases, the residual glass after devitrification would be enriched with nitrogen. The viscosity of the residual glass would be higher for the ZrO_2-containing glass-ceramic due to crystallization of more non-nitrogen containing crystalline phases. As nitrogen is known to stabilize these glasses, a residual glass richer in nitrogen would inhibit further crystal growth. Under these conditions it can be stated that ZrO_2 acts as a growth modifier during the crystal growth process. The intensity of the T_{c2} peak for the ZrO_2-containing glass after isothermal test becomes even lower compared with that for the ZrO_2-free glass (Figs 1, 6 and 7). This is again an indication of the lower crystallization rate of the ZrO_2-containing glass. Although the sectioned morphology of the ZrO_2-containing glass-ceramic shows the yttrium disilicate crystals to be embedded on zirconia, the fact that there are no obvious improvements in the volume fraction crystallization compared with the ZrO_2-free glass-ceramic suggests that the role of ZrO_2 in oxynitride glasses is not one of an effective nucleating agent. Lack of predominance of bulk nucleation seen during non-isothermal DSC runs for the ZrO_2 glass provides additional support to the above argument. Further, since the exact role of the Zr^{4+} cation in this silicate glass network is not known and no phase separation was observed, the lower activation energy obtained for the ZrO_2-containing glass can perhaps be attributed to the differences in the activation energies for crystallization of different crystal species in the ZrO_2-free and ZrO_2-containing glasses or to any structural reorganization that might have occurred by the stabilization of the zirconia structure. Since ZrO_2 addition to the oxynitride glass lowers the contribution of bulk crystallization to the overall crystallization, it appears that the essential role of zirconia in oxynitride glasses is one of a growth modifier rather than a nucleating agent.

5 Conclusions

Differential scanning calorimetry was used to determine the optimum nucleation temperature of ZrO_2-free and ZrO_2-containing oxynitride glasses. The results indicate that the optimum nucleation temperatures for the glasses with and without ZrO_2 are T_g + 50°C and T_g + 65°C, respectively. The activation energies for crystallization in the glasses calculated from the slope of the ln (α/T_p^2) versus $1/T_p$ plot indicated a lower value for the ZrO_2-containing glass due to the easier crystallization of a yttria-stabilized cubic zirconia phase. The influence of sample specific surface on the devitrification mechanisms has been estimated. Surface nucleation was found to be the dominant nucleation mechanism for both glass-ceramics. The essential role of zirconia in oxynitride glasses has been shown to be one of growth modifier rather than that of nucleating agent.

References

1. Jack, K. H., Sialon glasses. In *Nitrogen Ceramics*, ed. F.L. Riley. Noordhoof, The Hague, 1977, p. 257.
2. Shillito, K. R., Willis, R. R. & Bennett, R. B., Silicon metal oxynitride glasses. *J. Am. Ceram. Soc.*, **61**[11–12] (1978) 537.
3. Loehman, R. E., Preparation and properties of yttrium–silicon–aluminium oxynitride glasses. *J. Am. Ceram. Soc.*, **62**[9–10] (1979) 491.
4. Drew, R. A. L., Hampshire, S. & Jack, K. H., Nitrogen glasses. In *Special Ceramics 7*, eds P. Popper & D. E. Taylor. *Proc. Brit. Ceram. Soc.*, **31** (1981) 119.
5. Hampshire, S., Drew, R. A. L. & Jack, K. H., Viscosities, glass transition temperatures and microhardness of Y–Si– Al–O–N glasses. *J. Am. Ceram. Soc.*, **67** (1984) C46.
6. Ahn, C. C. & Thomas, G., Microstructure and grain boundary chemistry of hot pressed silicon nitride with yttria and alumina. *J. Am. Ceram. Soc.*, **66** (1983) 14.
7. Lewis, M. H., Mason, H. & Szweda, A., Syalon ceramic for application at high temperature and stress. In *Non-Oxide Technical and Engineering Ceramics*, ed. S. Hampshire. Elsevier-Applied Science Publishers, London, 1986, p. 175.
8. Leng-Ward, G. & Lewis, M. H., Crystallization in Y–Si–Al–O–N glasses. *Mater. Sci. Eng.*, **71** (1985) 101.
9. Dinger, T. R., Rai, R. S. & Thomas, G., Crystallization behaviour of a glass in the Y_2O_3–SiO_2–AlN system. *J. Am. Ceram. Soc.*, **71**[4] (1988) 236.
10. Hampshire, S., Oxynitride glasses and glass-ceramics. *Mater. Res. Soc. Symp. Proc.*, **287** (1993) 93.

11. Ramesh, R., Nestor, E., Pomeroy, M. J. & Hampshire, S., Optimisation of heat treatments for oxynitride glass-ceramics. *Key Eng. Mater.*, **99–100** (1995) 211.
12. Thomas, G., Ahn, C. & Weiss, J., Characterisation and crystallization of Y–Si–Al–O–N glass. *J. Am. Ceram. Soc.*, **65**[11] (1982) C-185.
13. Braue, W., Wotting, G. & Zeigler, G., Devitrification effect of grain boundary phases on high temperature strength of sintered Si_3N_4 materials. In *Ceramic Materials and Components for Engines*, eds W. Bunk & H. Hausner. Verlag Deutsche Keramische Gesellschaft, Bad Honnef, 1986, p. 503.
14. Cheng, Y. & Thompson, D. P., Nitrogen containing tetragonal zirconia. *J. Am. Ceram. Soc.*, **74** (1991) 1135.
15. Shaw, B. A., Cheng, Y. & Thompson, D. P., Nitrogen stabilization of tetragonal zirconias. *Brit. Ceram. Proc.*, **50** (1993) 143.
16. Vomacka, P., Babushkin, O. & Warren, R., Zirconia as a nucleating agent in an yttria–alumina–silica glass. *J. Eur. Ceram. Soc.*, **15** (1995) 1111–17.
17. Vomacka, P. & Babushkin, O., Yttria–alumina–silica glass with addition of zirconia. *J. Eur. Ceram. Soc.*, **15** (1995) 921.
18. Hampshire, S., Drew, R. A. L. & Jack, K. H., Oxynitride glasses. *Phys. Chem. Glasses*, **26** (1985) 182.
19. Marotta, A., Buri, A., Branda, F. & Saiello, S., Nucleation and crystallization of $Li_2O.2SiO_2$ glass—a DTA study. In *Advances in Ceramics*, eds J. H. Simmons, D. R. Uhlmann & B. H. Beall. American Ceramics Society, OH, 1982, p. 146.
20. Matusita, K. & Sakka, S., Kinetic study on crystallisation of glass by differential thermal analysis—criterion on application of Kissinger plot. *J. Non-Cryst. Solids*, **38&39** (1980) 741.
21. Donald, I. W., Metcalfe, B. L. & Morris, A. E. P., Influence of transition metal oxide additions on the crystallization kinetics, microstructures and thermal expansion characteristics of lithium zinc silicate glass. *J. Mater. Sci.*, **27** (1992) 2979.
22. Ekstrom, T., Falk, L. K. L. & Knutson-Wedel, E. M., Si_3N_4–ZrO_2 composites with small Al_2O_3 and Y_2O_3 additions prepared by HIP. *J. Mater. Sci.*, **26** (1991) 4331.